

RESEARCH ARTICLE

The influence of chemical modifications on the fragmentation behavior of fentanyl and fentanyl-related compounds in electrospray ionization tandem mass spectrometry

J. Tyler Davidson¹  | Zachary J. Sasiene²  | Glen P. Jackson^{1,2} 

¹Department of Forensic and Investigative Science, West Virginia University, Morgantown, WV, USA

²C. Eugene Bennett Department of Chemistry, West Virginia University, Morgantown, WV, USA

Correspondence

Glen P. Jackson, Department of Forensic and Investigative Science, West Virginia University, Morgantown, WV 26506-6121, USA.
Email: glen.jackson@mail.wvu.edu

Funding information

National Institute of Justice, Grant/Award Number: 2018-75-CX-0033

Abstract

Fentanyl is a synthetic opioid that has been approved by the FDA as a general anesthetic because of its rapid onset and high potency. However, since 2013 an opioid epidemic involving fentanyl or fentanyl-related compounds (FRCs) has swept the United States and caused numerous deaths in every state. The identification of novel FRCs is complicated by the rapid turnover of modifications to the core fentanyl structure. In this study, a series of 16 FRCs were analyzed using electrospray ionization tandem mass spectrometry (ESI-MS/MS) to gain a deeper understanding of the conserved and unique fragmentation behaviors associated with substitution to the core fentanyl structure. This work provides an approach, based on the product ions from ESI-MS/MS, to identify the modification site(s) on the core fentanyl structure for FRCs. Five common locations of substitution to the core fentanyl structure were used to assess the effect of substitution on the fragmentation behavior of FRCs. The proposed fragmentation pathways are supported through the combination of isotopic labeling, multi-stage mass spectrometry (MSⁿ), and accurate mass measurements with high-resolution mass spectrometry (HRMS). The identification of primary product ions specific to regions of substitution provides an additional tool for the identification of the location of substitution to the core fentanyl structure, which ultimately will assist toxicologists and seized drug analysts in the identification of emerging FRCs.

KEYWORDS

drug identification, fentanyl analogs, isotope labeling, tandem mass spectrometry

1 | INTRODUCTION

Fentanyl is a synthetic opioid that was first synthesized in 1960 by Paul Janssen.^{1,2} Due to its rapid onset and potency, fentanyl became a popular general anesthetic and was approved by the FDA in 1972 under the brand name Sublimaze.³ Fentanyl citrate (Sublimaze) was an intravenous anesthetic that was only available to clinicians and

surgeons. However, in the 1990s the introduction of transdermal fentanyl patches resulted in reports of misuse.^{1,4} In 1994, the FDA issued a warning about the dangers associated with fentanyl patches and the over-prescription of potent opioids.^{1,2} Unfortunately, fentanyl also began entering the drug market through clandestine laboratories and online suppliers who synthesized new analogs faster than could be controlled by the Drug Enforcement Administration (DEA).¹ In response, the DEA temporarily scheduled all non-classified FRCs as Schedule I narcotics to alleviate administrative and regulatory issues with prosecution.⁵ The two main routes of clandestine synthesis are

Funding information Grant number 2018-75-CX-0033, awarded by the National Institute of Justice, Office of Justice Programs, and U.S. Department of Justice.

the Janssen and Siegfried methods, with the Siegfried method – or a modified version thereof – being the most common method for clandestine synthesis.⁶

Very few fentanyl or FRC deaths were reported before 2013, and any reports were typically associated with heroin users. However, since 2013 an opioid epidemic has swept the United States and caused thousands of deaths involving FRCs.¹ In the US, there was a 259% increase in fentanyl seizures between 2013 and 2014, and the age-adjusted death rate increased by 80% for synthetic opioids, excluding methadone.² According to the 2017 and 2018 National Forensic Laboratory Information System (NFLIS) reports, there was an increase of more than 22,000 cases of fentanyl between 2016 and 2017 and more than 27,000 cases between 2017 and 2018.^{7,8}

Fentanyl and its synthetic precursors, such as 4-anilino-*N*-phenethylpiperidine (4-ANPP), are classified as Schedule II narcotics due to the medicinal value of fentanyl.^{1,6} However, fentanyl analogs such as α -methylfentanyl, 3-methylfentanyl, acetylfentanyl, butyrylfentanyl, and β -hydroxythiofentanyl lack medicinal approval and are listed as Schedule I narcotics.^{1–3} Figure 1 shows a generic chemical structure for FRCs, which highlights regions of common substitution. Modification sites include substitution of the aniline ring (R_1), loss or modification of the amide (R_2) and substitution on the piperidine ring (R_3), alkyl chain (R_4), or the monocyclic substituent (R_5), including phenyl, thiol, and tetrazole derivatives.

Because of its ubiquity, electron ionization-mass spectrometry (EI-MS) is frequently applied to the detection of FRCs, especially in combination with gas chromatography (GC). Ohta et al. analyzed 25 fentanyl derivatives and determined that 23 of the 25 compounds could be differentiated based on the combination of retention time on the GC and EI mass spectra, even in the absence of the molecular ion (M^+).⁹ Kanamori et al. analyzed a series of 3-methylfentanyl isomers and identified the conserved nature of the fragmentation pathways with the base peak of each spectrum corresponding with the cleavage of the benzyl moiety.¹⁰

The identification of novel FRCs has become so important that the National Institute of Standards and Technology (NIST) has developed an algorithm, known as the Hybrid Similarity Search (HSS) algorithm, that generates similarity scores based on both the fragment

ions and neutral losses so that structural modifications can be identified.¹¹ However, the HSS algorithm still struggles with the differentiation of positional isomers, which, if not chromatographically separated, must be differentiated manually using precise comparisons of relative ion abundances. For example, Mallette et al. demonstrated the differentiation of 2-methylfentanyl and 3-methylfentanyl using EI-MS, but differentiation was only possible based on the relative ion abundance of four fragment ions at m/z 216, 203, 202, and 160.¹² The DEA has also conducted work with cyclopropylfentanyl and crotonylfentanyl wherein the relative ion abundance of m/z 69 and m/z 105 was the criteria for differentiation.¹³ Recently, a more novel application of EI was demonstrated through the use of a field portable nano-liquid chromatography (nLC)-EI-MS for the detection of fentanyl analogs.¹⁴

Whereas EI-MS produces robust fragmentation that is conducive to mass spectral library searching, liquid chromatography (LC) introduction systems are also highly effective for the detection of FRCs in toxicology applications. LC introduction coupled to ESI or other ionization techniques can be used in conjunction with multiple reaction monitoring (MRM) for multiplex detection of a range of drugs and FRCs.^{15,16} LC introduction can also enable multiplex detection when combined with multi-stage mass spectrometry (MS^n)^{17,18} or accurate mass measurements with high-resolution mass spectrometry (HRMS).^{19,20} Another introduction method is ambient ionization, which involves the generation of gas-phase ions from untreated samples and reduces the need for extraction and chromatographic separation prior to tandem mass spectrometric analysis.²¹ Specifically, the application of direct analysis in real time (DART) ionization with HRMS has shown promising results for the identification of fentanyl and FRCs.^{22,23} Irrespective of sample introduction, tandem mass spectrometry benefits from the identification of both the molecular ion and the structural characterization through collision-induced dissociation (CID).

The conserved fragmentation behavior of FRCs can be very beneficial for the identification of novel FRCs, if the underlying fragmentation mechanisms can be understood. Examples of mechanistic interpretation for the generation of characteristic fentanyl fragmentation include Thevis et al.²⁴ Wichitnithad et al.²⁵ and our previous work on common intermediates in the tandem MS of FRCs.²⁶ However, these examples are focused on either fentanyl or specific FRCs, and as such do not provide a broad, generalized approach for the identification of the location of substitutions to the core fentanyl structure.

This study investigates the effect of substitution on the fragmentation behavior of fentanyl and FRCs in ESI-MS/MS with the goal of developing a general approach for the identification of the location of substitutions to the core fentanyl structure. The 16 FRCs analyzed in this study represent a variety of permutations of substitution in Figure 1. The use of isotopic labeling, MS^n , and accurate mass measurements with HRMS allows the determination of the direct relationship between each product ion (MS^n) and the elemental formula (HRMS). The use of isotopic labeling allows the labeled functionality to be followed down each fragmentation pathway as well as the identification of gas-phase rearrangements during CID. The use of both

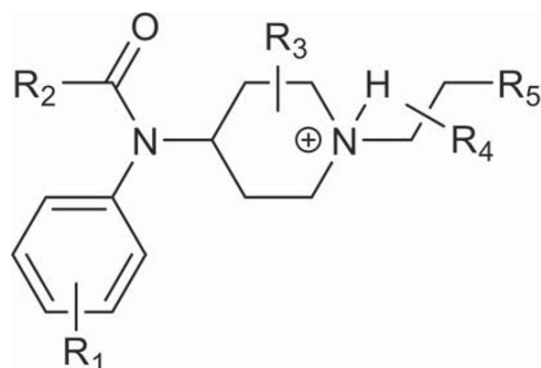


FIGURE 1 Generic chemical structure of fentanyl-related compounds (FRCs)

trapping and beam-type mass spectrometers also increases the applicability of these fragmentation pathways because the observations are common across different MS platforms. Finally, the ability to identify the location of substitution to the core fentanyl structure provides an additional tool to practitioners in the identification of emerging FRCs.

2 | METHODS

2.1 | Sample preparation

Thirteen FRC standards were purchased through Cayman Chemical (Ann Arbor, MI, USA), and three FRC standards were purchased through Cerilliant (Round Rock, TX, USA). The FRC standards purchased through Cayman Chemical were: 4-anilino-*N*-phenethylpiperidine (4-ANPP), fentanyl, fentanyl- d_5 , ortho-methylfentanyl, meta-methylfentanyl, cyclopropylfentanyl, crotonylfentanyl, para-methoxybutyrylfentanyl, methoxyacetylfentanyl, α -methylfentanyl, β -hydroxythiofentanyl- d_5 , $^{13}C_6$ -para-fluorofentanyl (labeled on the phenyl moiety), and $^{13}C_6$ -carfentanil (labeled on the phenyl moiety). The FRC standards purchased through Cerilliant were alfentanil, furanylfentanyl, and sufentanil- d_5 (perdeuterated on the amide). Ortho-methylfentanyl, meta-methylfentanyl, and $^{13}C_6$ -para-fluorofentanyl (labeled on the phenyl moiety) are examples of FRCs with substitution at location R_1 in Figure 1. Examples of FRCs with modification at location R_2 of Figure 1 include: 4-ANPP (loss of propionaldehyde), cyclopropylfentanyl, crotonylfentanyl, methoxyacetylfentanyl, and furanylfentanyl. $^{13}C_6$ -carfentanil, labeled on the phenyl moiety, is an example of a modification to location R_3 in Figure 1, whereas α -methylfentanyl is an example of a modification to location R_4 . Paramethoxybutyrylfentanyl, β -hydroxythiofentanyl- d_5 , alfentanil, and sufentanil- d_5 are examples of FRCs with a combination of modification locations, such as sufentanil- d_5 at location R_3 and R_5 of Figure 1. All non-deuterated standards were prepared in a solution of 49% HPLC grade methanol (Fisher Scientific, Palo Alto, CA, USA), 49% distilled water, and 2% acetic acid (Acros Organics, Pal Alto, CA, USA). The deuterated standards were prepared in HPLC grade methanol to reduce the risk of hydrogen back exchange. All solutions were prepared to a final concentration of approximately 100 ppm.

2.2 | Instrumentation

2.2.1 | Thermo Scientific Velos pro linear ion trap (LIT)

A heated-electrospray ionization source (HESI) was operated at 50°C with a spray voltage of 4000 V. Nitrogen gas was used for the sheath and auxiliary gas with a flow of 8 and 5 arbitrary units, respectively. The mass spectrometer capillary temperature was 275°C, and the scan range and normalized collision energy (NCE) were optimized for

each compound and are provided with each mass spectrum. An isolation width of 1 Da was used for all samples. Ultra-pure helium from Matheson TRIGAS (Fairmont, WV, USA) was used as the bath gas.

2.2.2 | Agilent Technologies 6538 UHD accurate-mass quadrupole time-of-flight (Q-TOF)

A dual ESI source was operated with a spray voltage of 3500 V and a 300°C nitrogen drying gas flow of 5 L/min and a nebulizer flow of 30 psig were used. The MS fragmentor and skimmer voltages, scan range, and collision energies were optimized for each compound and are labeled with each mass spectrum. An isolation width of 1.3 Da was used for all samples. Ultra-pure nitrogen was used for the collision gas purchased through Matheson TRIGAS (Fairmont, WV, USA).

2.3 | Data analysis

Xcalibur 2.0.0.48 software and MassHunter Qualitative Analysis B.05.00 were used for the Velos Pro and Agilent data analysis, respectively. Microsoft Excel version 14 (Microsoft, Redmond, WA, USA) and ChemDraw 16.0 (PerkinElmer, Waltham, MA, USA) were used for mass spectral plots and mass spectral fragmentation pathways.

2.3.1 | Mass spectral interpretation and mechanisms

Results from isotopic labeling, MS^n and accurate mass measurements with HRMS were combined to identify characteristic fragmentation pathways of FRCs. The complex nature of gas-phase mass spectral rearrangements can make it difficult to identify the exact hydrogen(s) involved in specific structural rearrangements. However, the ability to monitor specific functional groups using isotopic labeling provides deeper insight into which groups are retained and lost in a given fragmentation pathway.

2.4 | RESULTS AND DISCUSSION

The first phase of this project established several fragmentation pathways for protonated fentanyl and its main synthetic precursor 4-ANPP using tandem MS on a Q-TOF and a LIT.²⁶ The previous study confirmed the identity of three isobaric structures for the base peak at m/z 188 in MS^2 spectra of fentanyl; two of the structures were previously recognized by Wichitnithad et al.²⁵ and the third structure has a unique elemental composition and structure but the same nominal mass of m/z 188. The previous study also provided compelling evidence for an R-group transfer of the amide moiety to the N-atom of the piperidine ring during fragmentation.²⁶ The current study provides additional support for this unusual mechanism and shows that the mechanism is conserved for a range of FRCs.

The combination of the LIT and HRMS instruments permit the identification of the direct relationship between intermediate product ions. On the LIT, intermediates are identified via MS^n through sequential isolation and fragmentation events. The HRMS instrument allows the resolution of ions that are nominal isobars but have different exact masses. Examples are the product ions at m/z 188.1439 for $C_{13}H_{18}N^+$ and m/z 188.1075 for $C_{12}H_{14}NO^+$,^{25,26} which appear at the same nominal mass of m/z 188.1 in the LIT. For the purpose of this work, primary product ions are defined as product ions formed directly from the precursor ion without any intermediate ion between the precursor ion and primary product ion. Secondary and tertiary product ions are the result of subsequent fragmentation events from primary product ions. The relationships identified via the LIT instrument were then applied to the HRMS data collected on the Q-TOF instrument.

2.5 | HESI-Velos Pro MS^n

Figure 2 shows the MS^n fragmentation of ortho-methylfentanyl with the structures of the major fragments embedded. Isolation and fragmentation of the $[M+H]^+$ precursor at m/z 351 results in product ions at m/z 295, 230, 188, 146, and 105 (Figure 2A). The base peak of the tandem mass spectrum is observed at m/z 188, which is consistent with the two isobaric product ions formed through competing mechanisms for the loss of the *N*-phenylpropanamide neutral previously demonstrated by Wichitnithad et al.²⁵ The primary product ions at m/z 295 and m/z 230 are formed through the loss of methylketene (C_3H_4O) and phenethylamine ($C_8H_{11}N$), respectively, which are consistent with previous literature on the fragmentation of fentanyl.²⁶

Figure 2B shows the MS^4 product ion spectrum for the pathway m/z 351 \rightarrow 295 \rightarrow 188 \rightarrow . The product ions include m/z 160, 146, 132, and 105, which are formed through the loss of ethylene (C_2H_4), cyclopropane (C_3H_6), cyclobutene (C_4H_8), and tetrahydropyridine (C_5H_9N). Isolation and fragmentation of the intermediate product ion at m/z 230 results in the formation of product ions at m/z 202 and m/z 146, which are consistent with the methyl-substituted equivalents for fentanyl (Figure 2C).²⁶ The methyl-substituted structures appear 14 Da greater than the non-substituted analogs.

Figure 3 shows the MS^n fragmentation of methoxyacetylfentanyl with the major structural fragments embedded. The MS^2 spectrum is dominated by the intermediate product ion at m/z 188, which, like fentanyl, comprises at least two isobaric product ions (Figure 3A). The primary product ions observed at m/z 260 and m/z 232 correspond with the loss of aniline (C_6H_7N) and phenethylamine ($C_8H_{11}N$), which have been shown to be primary fragmentation pathways for fentanyl analogs.^{25,26} The primary product ion expected at m/z 281 is not observed for this compound. Recently, Nan et al. proposed that the presence of electron-accepting groups on the phenylalkylamide moiety eliminated the formation of this intermediate.²⁷

Figure 3B shows the isolation and fragmentation of the primary product ion at m/z 260, which results in a dominant product ion at m/z 206. The primary product ion at m/z 260 is formed through an R-group transfer from the aniline nitrogen to the piperidine nitrogen, as demonstrated previously for fentanyl.²⁶ The fragment at m/z 206 is formed through the loss of cyclobutene, which is observed for other FRCs wherein the novel R-group transfer is present. Finally, isolation and fragmentation of the primary product ion at m/z 232 results in dominant product ions at m/z 204 and m/z 176, which arise through the loss of ethylene (C_2H_4) and CO from the m/z 204 intermediate product ion (Figure 3C).

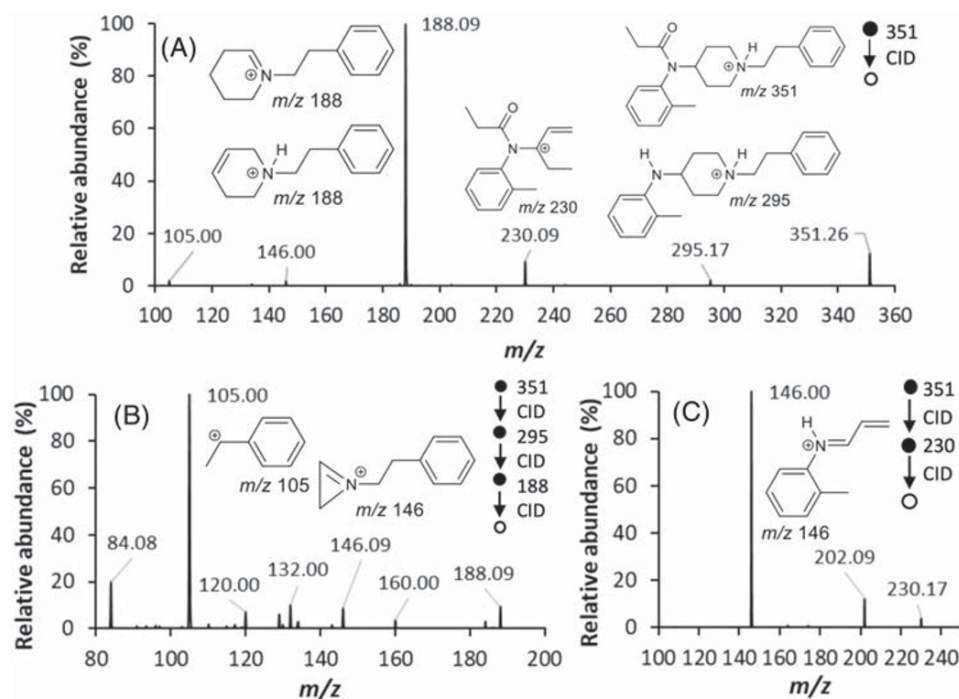
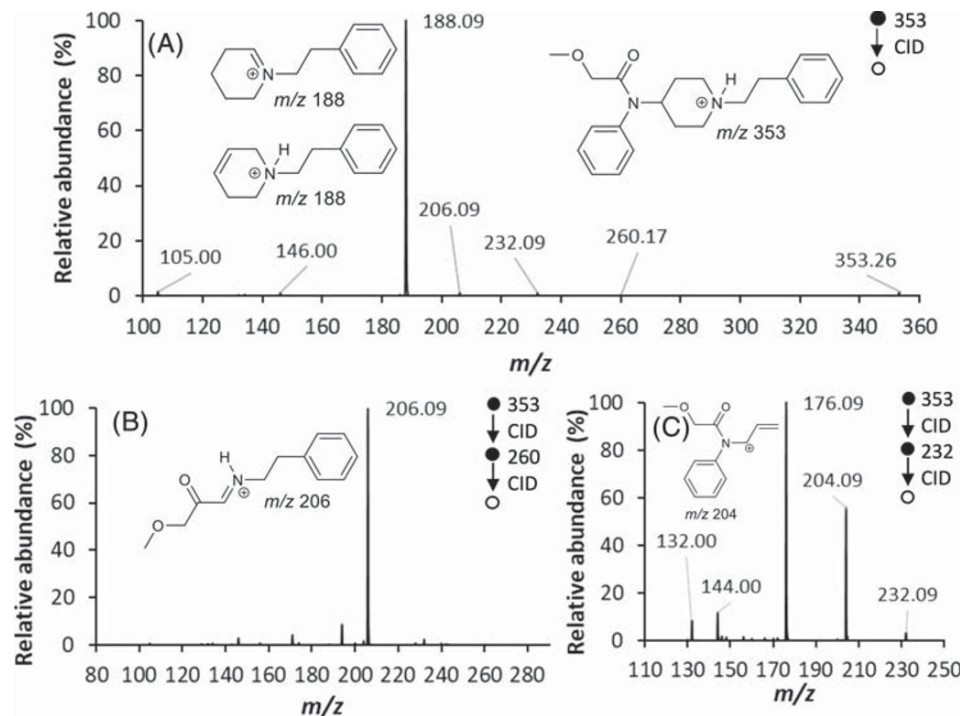


FIGURE 2 Tandem mass spectra of ortho-methylfentanyl: (A) MS^2 product ion spectrum of the $[M+H]^+$ molecular ion (30% NCE); (B) MS^4 product ion spectrum of the product ion at m/z 188 (35% NCE) showing the formation of product ions at m/z 160, 146, 132, and 105, among others; (C) MS^3 product ion spectrum of the primary product ion at m/z 230 (30% NCE) showing the formation of m/z 202 and m/z 146

FIGURE 3 Tandem mass spectra of methoxyacetyl-fentanyl: (A) MS² product ion spectrum of the [M+H]⁺ molecular ion (30% NCE); (B) MS³ product ion spectrum of the product ion at *m/z* 260 (30% NCE) showing the formation of a dominant product ion at *m/z* 206; (C) MS³ product ion spectrum of the primary product ion at *m/z* 232 (30% NCE) showing the formation of product ions at *m/z* 204, 176, 144, and 132

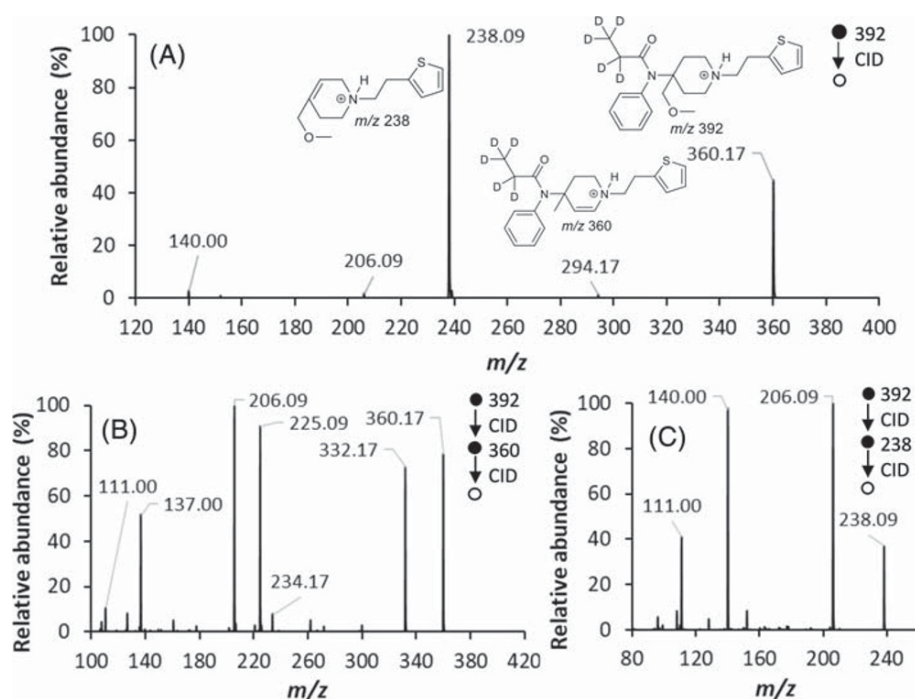


MSⁿ fragmentation of sufentanil-d₅ reveals an altered fragmentation pattern. Figure 4A demonstrates the dominance of two product ions at *m/z* 360 and *m/z* 238 in the MS² spectrum. Formation of the product ion at *m/z* 360 occurs through the loss of methanol (CH₄O) from the methoxymethylene substitution to the piperidine ring, which is analogous to the loss of methanol from the methyl ester functional group of carfentanil.²⁸ The base peak of the tandem mass spectrum of sufentanil-d₅ is at *m/z* 238 and occurs through the loss of the deuterated *N*-phenylpropanamide (C₉H₅D₅NO) without the presence of any

product ion through the loss of methylketene as observed for fentanyl at *m/z* 281.

As shown in Figure 4B, isolation and fragmentation of the primary product ion at *m/z* 360 of sufentanil-d₅ results in a large distribution of product ions including *m/z* 332, 225, 206, 137, and 111. The base peak of the MS³ spectrum for the pathway *m/z* 392 → 360 → is observed at *m/z* 206 (Figure 4B), which occurs through the loss of the deuterated *N*-phenylpropanamide (C₉H₅D₅NO), similar to the generation of the intermediate product ion at *m/z* 238 from the [M+H]⁺

FIGURE 4 Tandem mass spectra of sufentanil-d₅: (A) MS² product ion spectrum of the [M+H]⁺ molecular ion (30% NCE); (B) MS³ product ion spectrum of the product ion at *m/z* 360 (30% NCE) showing the formation of product ions at *m/z* 332, 234, 225, 206, 137, and 111, among others; (C) MS³ product ion spectrum of the primary product ion at *m/z* 238 (30% NCE) showing the formation of product ions at *m/z* 206, 140, and 111



precursor ion. Figure 4C is the MS³ spectrum for the pathway m/z 392 → 238→, which produces product ions at m/z 206, 140, and 111 with the base peak corresponding to the loss of methanol.

Figure 5 shows MSⁿ spectra of β -hydroxythiofentanyl-d₅ with the major structural fragments embedded. In the MS² spectrum in Figure 5A, the primary product ion at m/z 346 dominates the spectrum and must arise through the loss of H₂O, which is facilitated by the presence of the hydroxyl group on the alkyl chain. The only other primary product ion observed in the MS² spectrum is observed at m/z 250, which forms through the loss of hydroxymethylthiol. This fragmentation behavior is different in that the loss of H₂O is so dominant relative to the formation of any other primary product ions that the typical fragmentation pattern is obscured. Figure 5B shows the MS³ spectrum for the pathway m/z 364 → 346→, which results in product ions at m/z 286, 221, 207, 192, 158, and 147. The base peak at m/z 286 of the MS³ spectrum forms through the loss of deuterated methylketene. Figure 5C shows the MS³ spectrum for the pathway m/z 364 → 250→, which results in a variety of product ions, including m/z 207 and m/z 190, which form through piperidine ring enclosure and the loss of the deuterated methylketene moiety, respectively.

2.6 | Accurate-mass with HRMS Q-TOF

Accurate mass measurements of the compounds in Figures 1–4 confirm the elemental formulas for the proposed structures. As an example of this capability, Figure 6 shows the high-resolution tandem mass spectrum of para-methoxybutyrylfentanyl with the major structural fragments embedded. The primary product ions measured at m/z 311.2165 (expected at m/z 311.2123 for C₂₀H₂₇N₂O; 13 ppm error) and m/z 260.1663 (expected at m/z 260.1650 for C₁₆H₂₂NO₂; 5 ppm error) identify the elemental formulas shown in Figure 6. Formation of

the primary product ions at m/z 311.2165 and m/z 260.1663 occur through the loss of ethylketene (C₄H₆O) and phenethylamine (C₈H₁₁N), respectively. The accurate mass of the base peak of this spectrum at m/z 188.1455 (expected at m/z 188.1439 for C₁₃H₁₈N; 9 ppm error) is consistent with the structures shown in Figure 6. The conserved fragmentation pathways observed between the two instruments, and the consistency between the accurate mass measurements and theoretical exact masses, provides confidence that the proposed structures and pathways are typical observations in CID spectra of fentanyl analogs.

The HRMS tandem mass spectrum of alfentanil (Figure 7) highlights obvious differences in the fragmentation pathways relative to para-methoxybutyrylfentanyl (Figure 6) through the generation of primary product ions at m/z 385.2381 (expected at m/z 385.2351 for C₂₀H₂₉N₆O₂; 7 ppm error) and m/z 268.1831 (expected at m/z 268.1773 for C₁₂H₂₂N₅O₂; 21 ppm error). The primary product ions at m/z 385.2381 and m/z 268.1831 are formed through the loss of methanol (CH₄O) and *N*-phenylpropanamide (C₉H₁₀NO). These observations are consistent with sufentanil-d₅, which also contains a methoxymethylene substitution on the piperidine ring. The secondary product ion at m/z 314.1892 (expected at m/z 314.1868 for C₁₈H₂₄N₃O₂; 8 ppm error) forms through the loss of C₂H₅N₃ from the tetrazole functional group. This same C₂H₅N₃ loss from the tetrazole functional group also occurs from both the primary product ion at m/z 268.1831 and the secondary product ion at m/z 170.1061 (expected at m/z 170.1041 for C₆H₁₂N₅O; 12 ppm error) to form product ions at m/z 197.1345 (expected at m/z 197.1290 for C₁₀H₁₇N₂O₂; 28 ppm error) and m/z 99.0572 (expected at m/z 99.0558 for C₄H₇N₂O; 14 ppm error), respectively.

Figure 8 shows the HRMS tandem mass spectrum of α -methylfentanyl with proposed major structural fragments embedded. The base peak of this spectrum is observed at m/z 91.0580,

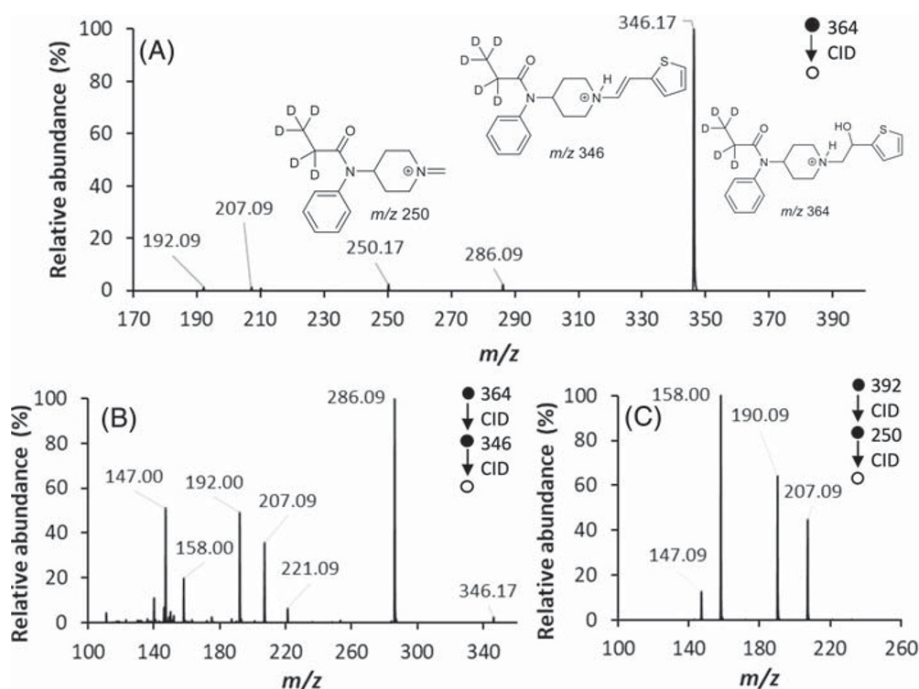


FIGURE 5 Tandem mass spectra of β -hydroxythiofentanyl-d₅: (A) MS² product ion spectrum of the [M + H]⁺ molecular ion (30% NCE); (B) MS³ product ion spectrum of the product ion at m/z 346 (30% NCE) showing the formation of product ions at m/z 286, 221, 207, 192, 158, and 147, among others; (C) MS³ product ion spectrum of the primary product ion at m/z 250 (30% NCE) showing the formation of product ions at m/z 207 and m/z 190, among others

FIGURE 6 Tandem mass spectrum of paramethoxybutrylfentanyl collected with a 25 eV collision energy, 250 V fragmentor voltage and 65 V skimmer voltage

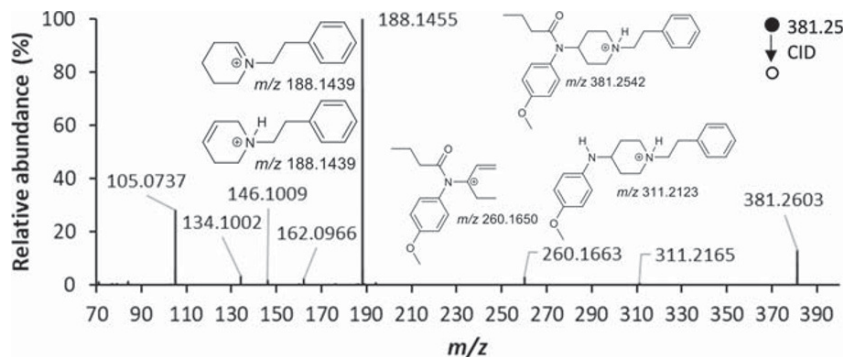


FIGURE 7 Tandem mass spectrum of alfentanil collected with a 25 eV collision energy, 225 V fragmentor voltage and 65 V skimmer voltage

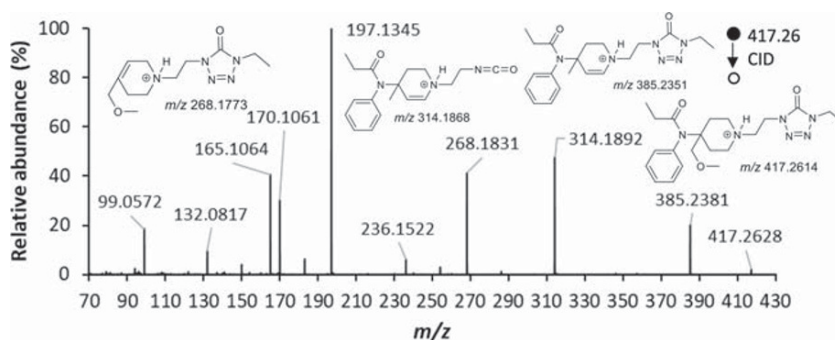
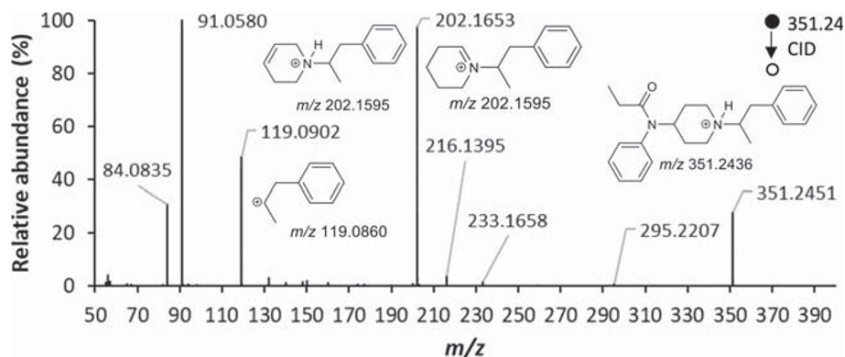


FIGURE 8 Tandem mass spectrum of α -methylfentanyl collected with a 25 eV collision energy, 250 V fragmentor voltage and 65 V skimmer voltage



consistent with the elemental formula $C_7H_7^+$, commonly referred to as the tropylium ion. The presence of the methyl group on the α -carbon leads to the formation of the intermediate ion at m/z 119.0902 (expected at m/z 119.0860 for C_9H_{11} ; 35 ppm error), which readily fragments into the tropylium ion.

The other dominant product ion at m/z 202.1653 (expected at m/z 202.1595 for $C_{14}H_{20}N$; 29 ppm error) is consistent with the methyl-substituted derivative of the m/z 188.1439 base peak for non-piperidine ring substituted fentanyl analogs. The primary product ions at m/z 295.2207 (expected at m/z 295.2174 for $C_{20}H_{27}N_2$; 11 ppm error) and m/z 216.1395 (expected at m/z 216.1388 for $C_{14}H_{18}NO$; 3 ppm error) are formed through the loss of methylketene (C_3H_4O) and 2-phenylpropylamine ($C_9H_{13}N$), respectively. The only other primary product ion of any meaningful abundance is observed at m/z 233.1658 (expected at m/z 233.1653 for $C_{14}H_{21}N_2O$; 2 ppm error), which forms through the loss of a phenylpropyl neutral that is facilitated by the presence of the methyl group on the α -carbon.

Supplemental Figure 1 contains the HRMS tandem mass spectrum of $^{13}C_6$ -carfentanil with the major structural fragments embedded. The $[M+H]^+$ precursor at m/z 401.2495 (expected at m/z 401.2535 for $C_{18}^{13}C_6H_{31}N_2O_3$; 10 ppm error) fragments into primary product ions at m/z 369.2115 (expected at m/z 369.2273 for $C_{17}^{13}C_6H_{27}N_2O_2$; 42 ppm error) and m/z 341.2345 (expected at m/z 341.2324 for $C_{16}^{13}C_6H_{27}N_2O$; 6 ppm error). The secondary product ion at m/z 252.1754 (expected at m/z 252.1695 for $C_9^{13}C_6H_{20}NO_2$; 23 ppm error) forms through the elimination of *N*-phenylpropanamide ($C_9H_{16}NO$), which ultimately forms tertiary product ions at m/z 192.1504 (expected at m/z 192.1484 for $C_7^{13}C_6H_{16}N$; 10 ppm error), m/z 140.1201 (expected at m/z 140.1171 for $C_3^{13}C_6H_{16}N$; 21 ppm error) and m/z 113.0634 (expected at m/z 113.0602 for $C_6H_9O_2$; 28 ppm). The secondary product ion at m/z 285.2077 (expected at m/z 285.2062 for $C_{13}^{13}C_6H_{23}N_2$; 5 ppm error) forms through the loss of methylketene and forms tertiary product ions at m/z 192.1504 (expected at m/z 192.1484 for $C_7^{13}C_6H_{16}N$; 10 ppm error) and m/z 146.1009 (expected at m/z 146.0969 for $C_{10}H_{12}N$; 27 ppm error).

Scheme 1 shows the observed primary product ions for FRCs with ESI-MS/MS based on the use of isotopic labeling, MSⁿ, and HRMS. The eight fragmentation pathways highlight the effect of substitution to the core fentanyl structure on the observed primary product ions, with each location of substitution directing unique fragmentation pathways. Based on the FRCs analyzed, substitution to the aniline ring (R₁) and amide moiety (R₂) does not alter the fragmentation mechanisms relative to fentanyl with the lone exceptions being methoxyacetylfentanyl (Figure 3) and furanylfentanyl, both of which show reduced abundance for pathway 5, likely due to the electron-accepting characteristics of the amide moiety (R₂) substitutions.²⁷ Pathways 6 and 7 are still observed for methoxyacetylfentanyl and furanylfentanyl and, in fact, the altered fragmentation mechanism seems to enhance the formation of product ions through pathway 7.

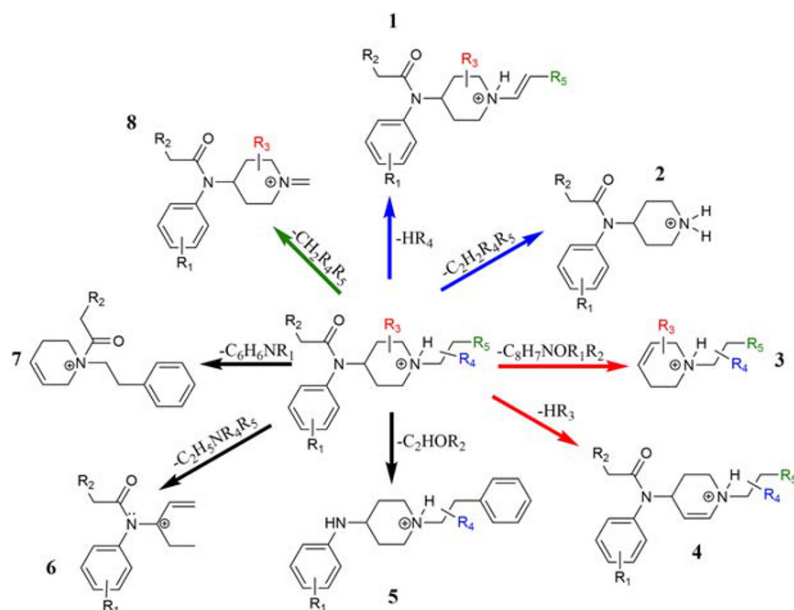
In general, pathways 5, 6, and 7 are more frequently observed for FRCs with substitution to the aniline ring (R₁) and amide (R₂) moieties, which is consistent with the fragmentation behavior of fentanyl. Pathway 5 occurs through the loss of a substituted-ketene from the protonated precursor and pathway 6 arises through the opening of the piperidine ring and charge stabilization on a tertiary carbocation. Whereas pathways 5 and 6 are the dominant primary product ions observed in the protonated tandem mass spectra for R₁ and R₂ substituted FRCs, the product ions of pathway 7 are often observable at ~1% the abundance of the base peak.

The presence of a substituent on the piperidine ring (R₃) favors pathways 3 and 4. Pathway 3 occurs through the direct loss of *N*-phenylpropanamide (C₉H₁₀NO), whereas pathway 4 arises through the loss of either a portion or the entire functional group on the piperidine ring (R₃). The piperidine ring-substituted FRCs analyzed in this study were all substituted in the 4-position of the piperidine ring and, as such, the fragmentation behavior described for pathway 3 is only applicable to the 4-position substitutions. A recent study by Nan et al. demonstrated that piperidine ring substitutions in the 3-position do not display the characteristic behavior of piperidine

ring substitutions in the 4-position.²⁷ Note that pathway 3 involves the direct cleavage of the *N*-phenylpropanamide moiety—with the absence of any evidence of any intermediate—through the loss of methylketene, as observed for pathway 5. Examples for pathway 3 include nominal *m/z* 238 for sufentanil-d₅ (Figure 4), nominal *m/z* 268 for alfentanil (Figure 7), and nominal *m/z* 252 for ¹³C₆-carfentanil (Supplemental 1).

The FRCs analyzed in this study were substituted in the 4-position of the piperidine ring with either methoxymethylene or carboxymethylester functional groups. The methoxymethylene substituted compounds favored pathway 4 through the loss of methanol as observed for product ions at nominal *m/z* 385 for alfentanil (Figure 7) and nominal *m/z* 360 for sufentanil-d₅ (Figure 4). In comparison, the carboxymethylester substituted compounds, such as ¹³C₆-carfentanil (Supplemental 1) demonstrated both the loss of methanol (i.e. *m/z* 369) and the loss of methyl formate (i.e. *m/z* 341). This fragmentation behavior may be specific to carboxymethylester compounds, which would provide an additional method of the identification of carboxymethylester substituted novel FRCs. The position of the double bond in the piperidine ring of pathway 4 is specific to the compounds analyzed in this study, and the position is likely to change depending on the position of the substituents.

The fragmentation pathways for FRCs with substitution to the alkyl chain (R₄) are controlled by the composition of the substitution at R₄. For example, pathway 1 in Scheme 1 is the dominant fragmentation pathway for FRCs with a hydroxyl group at location R₄, as seen by the peak at *m/z* 346 for β-hydroxythiofentanyl-d₅ (Figure 5). In contrast, pathway 2 is favored with R₄ as an aliphatic substitution on the α-carbon, as visualized by the product ion at *m/z* 233 for α-methylfentanyl (Figure 8). Despite the presence of an R₄ functional group to provide additional fragmentation products to the tandem mass spectrum of a FRC, certain product ions – such as those at *m/z* 119 and *m/z* 91, which form through secondary and tertiary fragmentation along pathway 5 – are far more dominant than any of the



SCHEME 1 Observed primary product ions for FRCs with ESI-MS/MS. The color of an R group indicates that it tends to direct fragmentation down a pathway of the same color [Colour figure can be viewed at wileyonlinelibrary.com]

fragments of pathway 2, including the primary product ion at m/z 233 for α -methylfentanyl in Figure 8. The product ions at m/z 119 and m/z 91 for α -methylfentanyl (Figure 8) were confirmed to derive mainly through pathway 5 using MS³ of the various primary product ions for α -methylfentanyl. In summary, the presence of aliphatic groups on the alpha carbon (R_4) enable the observation of products through pathways 1 and 2, but these fragments are typically minor relative to the consecutive fragments of other pathways.

As demonstrated in the last example for α -methylfentanyl, the abundance of a primary fragment ion of a pathway is not the only, or the most reliable, measure of the favorability of a fragmentation pathway. Instead, to determine the relative favorability of a pathway, we relied on MS³ spectra to determine the most abundant consecutive fragments of a pathway, and we used the sum of the product ion abundances of each spectrum to assess the relative favorability of each fragment. Therefore, although the abundance of a high mass primary product ion such as m/z 233 for pathway 2 for α -methylfentanyl might not increase much when its formation is favored by the methyl group, the low mass consecutive fragments that derive from it, such as m/z 84, do show a more dramatic increase in abundance because of the additional functionality.

Pathway 8 occurs through the loss of the substitution or a portion of the substitution to location R_5 . Examples of this pathway include m/z 250 for β -hydroxythiofentanyl-d₅ (Figure 5) wherein the whole R_5 substitution is lost and m/z 314 for alfentanil (Figure 7), which demonstrates the loss of only a portion of the tetrazole substituent.

Table 1 provides a summary of the five most abundant product ions in the MS² spectra of the $[M+H]^+$ protonated precursor for the

16 FRCs analyzed in this study. The table contains both LIT data and Q-TOF data, and the peaks are ordered according to their decreasing relative abundance. Whereas the five most abundant peaks contain a great deal of overlap between the two instruments, the Q-TOF product ion spectra often contain more abundant ions with lower m/z values relative to the LIT data. These abundances stem from the differences in activation timescales and energies between the two instruments, and the knowledge that beam-type CID in the Q-TOF instrument provides more rapid and higher energy activation, which ultimately encourages additional consecutive fragmentation relative to the slow heating of the LIT.^{29–33}

Table 1 emphasizes the following important FRC behaviors: (1) the five most abundant product ions in the tandem mass spectra are most often either the primary product ions identified in Scheme 1 or secondary/tertiary fragmentation thereof, (2) the five most abundant product ions are relatively conserved between the trapping (LIT) and beam-type (Q-TOF) mass spectrometers, and (3) if one takes into account the mass of the functional groups, the most abundant pathways and fragments are generally conserved between FRCs. For example, the base peak at m/z 188 for the first nine compounds in the table follow pathway 5. The same pathway forms the base peak at m/z 202 for α -methylfentanyl and m/z 194 for ¹³C₆-para-fluorofentanyl, for example. There are also several situations where product ions can be formed through two competing pathways, such as the product ion at m/z 111 for sufentanil-d₅ through pathways 3 and 4. The real impact of this knowledge is that the product ions formed from ESI-MS/MS can be used to identify the mass and location of substitutions based on shifts in mass due to the additional substituent. However, we recognize that the use of this knowledge

TABLE 1 Protonated precursor ion mass-to-charge values and five most abundant product ions in decreasing order of relative abundance for each compound in this study with the LIT and Q-TOF instruments

Compound	$[M+H]^+$	LIT product ions (m/z) @30% NCE	Q-TOF product ions (m/z) @25 eV
4-ANPP	m/z 281	188 ^{5#} , 134 ^{5#} , 105 ^{5#} , 146 ^{5#} , 120 ^{5#}	105.07 ^{5#} , 188.14 ^{5#} , 134.09 ^{5#} , 146.09 ^{5#} , 84.08
Fentanyl	m/z 337	188 ^{5/6#} , 281 ⁵ , 216 ⁶ , 105 ^{5#} , 146 ^{5#}	188.14 ^{5/6#} , 105.07 ^{5#} , 216.13 ⁶ , 134.09 ^{5#} , 146.09 ^{5#}
Fentanyl-d ₅	m/z 342	188 ^{5#} , 286 ⁵ , 221 ⁶ , 105 ^{5#} , 146 ^{5#}	188.14 ^{5#} , 105.07 ^{5#} , 221.16 ⁶ , 134.09 ^{5#} , 146.09 ^{5#}
Ortho-methylfentanyl	m/z 351	188 ^{5#} , 230 ⁶ , 146 ^{5/6#} , 295 ⁵ , 105 ^{5#}	188.14 ^{5#} , 105.07 ^{5#} , 146.09 ^{5/6#} , 230.15 ⁶ , 134.09 ^{5#}
Meta-methylfentanyl	m/z 351	188 ^{5#} , 230 ⁶ , 295 ⁵ , 105 ^{5#} , 146 ^{5/6#}	188.14 ^{5#} , 105.07 ^{5#} , 146.09 ^{5/6#} , 134.09 ^{5#} , 230.15 ⁶
Cyclopropylfentanyl	m/z 349	188 ^{5#} , 281 ⁵ , 228 ⁶ , 105 ^{5#} , 146 ^{5#}	188.14 ^{5#} , 105.07 ^{5#} , 69.03, 134.09 ^{5#} , 228.13 ⁶
Crotonylfentanyl	m/z 349	188 ^{5#} , 281 ⁵ , 228 ⁶ , 105 ^{5#} , 146 ^{5#}	188.14 ^{5#} , 105.07 ^{5#} , 69.03, 134.09 ^{5#} , 228.13 ⁶
Para-methoxybutyrylfentanyl	m/z 381	188 ^{5#} , 260 ⁶ , 311 ⁵ , 146 ^{5#} , 134 ^{5#}	188.14 ^{5#} , 105.07 ^{5#} , 134.09 ^{5#} , 260.16 ⁶ , 162.09 ^{6#}
Methoxyacetyl fentanyl	m/z 353	188 ⁵ , 105 ^{5#} , 206 ^{7#} , 232 ⁶ , 146 ^{5#}	188.14 ⁵ , 105.07 ^{5#} , 134.09 ^{5#} , 146.09 ^{5#} , 84.08
α -Methylfentanyl	m/z 351	202 ^{5#} , 216 ⁶ , 119 ^{5#} , 233 ² , 295 ⁵	202.15 ^{5#} , 91.05 ^{5#} , 119.08 ^{5#} , 84.08, 216.13 ⁶
β -Hydroxythiofentanyl-d ₅	m/z 364	346 ¹ , 250 ⁸ , 286 ^{1#} , 192 ^{1#} , 207 ^{1#}	192.08 ^{1#} , 97.01, 346.19 ¹ , 147.10 ^{1#} , 111.02
¹³ C ₆ -Para-fluorofentanyl	m/z 361	194 ^{5#} , 234 ⁶ , 305 ⁵ , 111 ^{5#} , 152 ^{5#}	194.16 ^{5#} , 111.09 ^{5#} , 140.11 ^{5#} , 234.12 ⁶ , 152.11 ^{5#}
¹³ C ₆ -Carfentanil	m/z 401	369 ⁴ , 341 ⁴ , 252 ^{5#} , 220 ^{5#} , 285 ^{4#}	113.06 ^{5#} , 252.16 ^{5#} , 341.23 ⁴ , 140.11 ^{5#} , 285.20 ^{4#}
Alfentanil	m/z 401	268 ³ , 385 ⁴ , 197 ^{3#} , 170 ^{3#} , 236 ^{3#}	197.12 ^{3#} , 314.18 ^{4#} , 268.17 ³ , 165.10 ^{3/4#} , 170.10 ^{3#}
Furanylfentanyl	m/z 375	188 ³ , 146 ^{3#} , 254 ⁶ , 228 ^{7#} , 134 ^{3#}	188.14 ³ , 105.07 ^{3#} , 146.09 ^{3#} , 134.09 ^{3#} , 84.08
Sufentanil-d ₅	m/z 392	238 ³ , 360 ⁴ , 140 ^{3#} , 206 ^{4#} , 294 ⁸	238.12 ³ , 111.02 ^{3/4#} , 360.21 ⁴ , 140.10 ^{3#} , 206.09 ^{4#}

^{*}Superscripts correspond with the primary product ion pathway from Scheme 1.

[#]Indicates secondary or tertiary fragmentation from the indicated primary product ion in Scheme 1.

currently requires extensive manual interpretations, and that most practitioners will struggle to apply these general trends. The toxicology and seized drug communities could benefit from an automated spectral similarity search, similar to the HSS algorithm for EI spectra that was applicable to tandem mass spectra of protonated FRCs. Until then, analysts will have to rely on manual interpretations following a generalized set of rules – such as those proposed here – to identify emerging FRCs.

3 | CONCLUSIONS

The combination of isotopic labeling, MSⁿ, and accurate mass measurements with HRMS was used to develop general rules for the fragmentation of fentanyl analogs and the identification of substitutions to the core fentanyl structure. A series of 16 FRCs with substitutions at five common locations to the core fentanyl structure was used to identify general fragmentation pathways and their propensity to direct fragmentation down particular pathways. The identification of primary product ions for FRCs substituted at each of the five locations of substitution as well as the relative consistency of the five most abundant product ions between the LIT and Q-TOF instruments provides guidance to the forensic community about how to identify the location of substitution for FRCs that is applicable across different MS platforms. Finally, the identification of the conserved fragmentation pathways, when accounting for differences in the mass and location of the substituent for FRCs, provides an additional tool for the identification of novel FRCs to toxicologists and seized drug analysts.

ACKNOWLEDGMENTS

This project was supported by grant number 2018-75-CX-0033, awarded by the National Institute of Justice, Office of Justice Programs, and U.S. Department of Justice. The opinions, findings, and conclusions or recommendations expressed in this publication are those of the authors and do not necessarily reflect the views of the Department of Justice.

ORCID

J. Tyler Davidson  <https://orcid.org/0000-0001-9932-8273>

Zachary J. Sasiene  <https://orcid.org/0000-0001-6020-3828>

Glen P. Jackson  <https://orcid.org/0000-0003-0803-6254>

REFERENCES

- Armenian P, Vo KT, Barr-Walker J, Lynch KL. Fentanyl, fentanyl analogs and novel synthetic opioids: a comprehensive review. *Neuropharmacology*. 2018;134(Pt A):121-132. <https://doi.org/10.1016/j.neuropharm.2017.10.016>
- Suzuki J, El-Haddad S. A review: fentanyl and non-pharmaceutical fentanyls. *Drug Alcohol Depend*. 2017;171:107-116. <https://doi.org/10.1016/j.drugalcdep.2016.11.033>
- Schueler HE. Emerging synthetic fentanyl analogs. *Acad Forensic Pathol*. 2017;7(1):36-40. <https://doi.org/10.23907/2017.004>
- Rose PG, Macfee MS, Boswell MV. Fentanyl transdermal system overdose secondary to cutaneous hyperthermia. *Anesth Analg*. 1993;77(2):390-391.
- Drug Enforcement Administration, Department of Justice. Schedules of controlled substances: temporary placement of fentanyl related substances in schedule I. *Fed Regist*. 2018;83(25):5188–5192.
- Control of immediate precursor used in the illicit manufacture of fentanyl as a schedule II controlled substance. *Fed Regist*. 2010;75(124):37295–37299.
- NFLIS-DRUG 2017 Annual Report. U.S. Department of Justice Drug Enforcement Administration: National Forensic Laboratory Information System (NFLIS) 2017.
- NFLIS-Drug 2018 Annual Report. U.S. Department of Justice Drug Enforcement Administration: National Forensic Laboratory Information System (NFLIS) 2018.
- Ohta H, Suzuki S, Ogasawara K. Studies on fentanyl and related compounds IV. Chromatographic and spectrometric discrimination of fentanyl and its derivatives. *J Anal Toxicol*. 1999;23(4):280-285.
- Kanamori T, Iwata YT, Segawa H, et al. Characterization and differentiation of geometric isomers of 3-methylfentanyl analogs by gas chromatography/mass spectrometry, liquid chromatography/mass spectrometry, and nuclear magnetic resonance spectroscopy. *J Forensic Sci*. 2017;62(6):1472-1478. <https://doi.org/10.1111/1556-4029.13395>
- Moorthy AS, Wallace WE, Kearsley AJ, Tchekhovskoi DV, Stein SE. Combining fragment-ion and neutral-loss matching during mass spectral library searching: a new general purpose algorithm applicable to illicit drug identification. *Anal Chem*. 2017;89(24):13261-13268. <https://doi.org/10.1021/acs.analchem.7b03320>
- Mallette JR, Casale JF, Toske SG, Hays PA. Characterization of (2R,4S)- and (2R,4R)-2-methylfentanyl and their differentiation from cis- and trans -3-methylfentanyl. *Forensic Chem*. 2018;8:64-71. <https://doi.org/10.1016/j.forc.2018.02.001>
- Mallette JR, Casale JF, Hays PA. Characterization and differentiation of cyclopropylfentanyl from E-crotonylfentanyl, Z-crotonylfentanyl, and 3-butenylfentanyl. *Sci Justice*. 2019;59(1):67-74.
- Abonamah JV, Eckenrode BA, Moini M. On-site detection of fentanyl and its derivatives by field portable nano-liquid chromatography-electron ionization-mass spectrometry (nLC-EL-MS). *Forensic Chem*. 2019;16:100180. <https://doi.org/10.1016/j.forc.2019.100180>
- Strayer KE, Antonides HM, Juhascik MP, Daniulaityte R, Sizemore IE. LC-MS/MS-based method for the multiplex detection of 24 fentanyl analogues and metabolites in whole blood at sub ng mL⁻¹ concentrations. *J Am Chem Soc*. 2018;3(1):514-523. <https://doi.org/10.1021/acsomega.7b01536>
- Lurie IS, Iio R. Use of multiple-reaction monitoring ratios for identifying incompletely resolved fentanyl homologs and analogs via ultra-high-pressure liquid chromatography-tandem mass spectrometry. *J Chromatogr A*. 2009;1216(9):1515-1519. <https://doi.org/10.1016/j.chroma.2008.12.097>
- Shoff EN, Zaney ME, Kahl JH, Hime GW, Boland DM. Qualitative identification of fentanyl analogs and other opioids in postmortem cases by UHPLC-ion trap-MSⁿ. *J Anal Toxicol*. 2017;41(6):484-492. <https://doi.org/10.1093/jat/bkx041>
- Rittgen J, Putz M, Zimmermann R. Identification of fentanyl derivatives at trace levels with nonaqueous capillary electrophoresis-electrospray-tandem mass spectrometry (MSⁿ, n = 2, 3): analytical method and forensic applications. *Electrophoresis*. 2012;33(11):1595-1605. <https://doi.org/10.1002/elps.201100655>
- Breindahl T, Kimergard A, Andreassen MF, Pedersen DS. Identification of a new psychoactive substance in seized material: the synthetic opioid N-phenyl-N-[1-(2-phenethyl)piperidin-4-yl]prop-2-enamide (Acrylfentanyl). *Drug Test Anal*. 2017;9(3):415-422. <https://doi.org/10.1002/dta.2046>
- Noble C, Weihe Dalsgaard P, Stybe Johansen S, Linnet K. Application of a screening method for fentanyl and its analogues using UHPLC-QTOF-MS with data-independent acquisition (DIA) in MS^E mode and

- retrospective analysis of authentic forensic blood samples. *Drug Test Anal.* 2018;10(4):651-662. <https://doi.org/10.1002/dta.2263>
21. Ferreira CR, Yannell KE, Jarmusch AK, Pirro V, Ouyang Z, Cooks RG. Ambient ionization mass spectrometry for point-of-care diagnostics and other clinical measurements. *Clin Chem.* 2016;62(1):99-110. <https://doi.org/10.1373/clinchem.2014.237164>
 22. Sisco E, Verkouteren J, Staymates J, Lawrence J. Rapid detection of fentanyl, fentanyl analogues, and opioids for on-site or laboratory based drug seizure screening using thermal desorption DART-MS and ion mobility spectrometry. *Forensic Chem.* 2017;4:108-115. <https://doi.org/10.1016/j.forc.2017.04.001>
 23. Moore A, Foss J, Juhascik M, Botch-Jones S, Kero F. Rapid screening of opioids in seized street drugs using ambient ionization high resolution time-of-flight mass spectrometry. *Forensic Chem.* 2019;13:100149. <https://doi.org/10.1016/j.forc.2019.100149>
 24. Thevis M, Geyer H, Bahr D, Schanzer W. Identification of fentanyl, alfentanil, sufentanil, remifentanil and their major metabolites in human urine by liquid chromatography/tandem mass spectrometry for doping control purposes. *Eur J Mass Spectrom.* 2005;11(4):419-427. <https://doi.org/10.1255/ejms.761>
 25. Wichitnithad W, McManus TJ, Callery PS. Identification of isobaric product ions in electrospray ionization mass spectra of fentanyl using multistage mass spectrometry and deuterium labeling. *Rapid Commun Mass Spectrom.* 2010;24(17):2547-2553. <https://doi.org/10.1002/rcm.4673>
 26. Davidson JT, Sasiene ZJ, Jackson GP. The characterization of isobaric product ions of fentanyl using multi-stage mass spectrometry, high-resolution mass spectrometry and isotopic labeling. *Drug Test Anal.* 2020;12(4):496-503. <https://doi.org/10.1002/dta.2758>
 27. Nan Q, Hejian W, Ping X, et al. Investigation of fragmentation pathways of fentanyl analogues and novel synthetic opioids by electron ionization high-resolution mass spectrometry and electrospray ionization high-resolution tandem mass spectrometry. *J Am Soc Mass Spectrom.* 2020;31(2):277-291. <https://doi.org/10.1021/jasms.9b00112>
 28. Feasel MG, Wohlfarth A, Nilles JM, Pang S, Kristovich RL, Huestis MA. Metabolism of carfentanil, an ultra-potent opioid, in human liver microsomes and human hepatocytes by high-resolution mass spectrometry. *AAPS J.* 2016;18(6):1489-1499. <https://doi.org/10.1208/s12248-016-9963-5>
 29. McLuckey SA. Principles of collisional activation in analytical mass spectrometry. *J Am Soc Mass Spectrom.* 1992;192(3):599-614.
 30. McMahon TB. Thermochemical ladders: scaling the ramparts of gaseous ion energetics. *Int J Mass Spectrom.* 2000;200:187-199.
 31. Sleno L, Volmer DA. Ion activation methods for tandem mass spectrometry. *J Mass Spectrom.* 2004;39(10):1091-1112. <https://doi.org/10.1002/jms.703>
 32. McLuckey SA, Goeringer DE. Slow heating methods in tandem mass spectrometry. *J Mass Spectrom.* 1997;32:461-474.
 33. Wells JM, McLuckey SA. Collision-induced dissociation (CID) of peptides and proteins. In: Burlingame AL, ed. *Methods in enzymology*; 2005:148-185.

SUPPORTING INFORMATION

Additional supporting information may be found online in the Supporting Information section at the end of this article.

How to cite this article: Davidson JT, Sasiene ZJ, Jackson GP. The influence of chemical modifications on the fragmentation behavior of fentanyl and fentanyl-related compounds in electrospray ionization tandem mass spectrometry. *Drug Test Anal.* 2020;12:957-967. <https://doi.org/10.1002/dta.2794>